PNAS RESEARCH ARTICLE | NEUROSCIENCE OPEN ACCESS

Keratinocyte–TRPV1 sensory neuron interactions in a genetically controllable mouse model of chronic neuropathic itch

Andrew J. Crowther[a,1], Sakeen W. Kashem[b,c,1], Madison E. Jewell[a], Henry Le Chang[a], Élora Midavaine[a], Mariela Rosa Casillas[a], Veronika Danchine[b], Sian Rodriguez[a], Artur Kania[d], Ritchie Chen[e], Joao M. Braz[a], and Allan I. Basbaum[a,2]

Edited by Peter Strick, University of Pittsburgh Brain Institute, Pittsburgh, PA; received June 13, 2024; accepted May 5, 2025

Our understanding of neural circuits that respond to skin dysfunction, triggering itch, and pathophysiological scratching remains incomplete. Here, we describe a profound chronic itch phenotype in transgenic mice expressing the tetracycline transactivator (tTA) gene within the Phox2a lineage. Phox2a; tTA mice exhibit intense, localized scratching and regional skin lesions, controllable by the tTA inhibitor, doxycycline. As gabapentin and the kappa opioid receptor agonist, nalfurafine, but not morphine, significantly reduce scratching, this phenotype has a pharmacological profile of neuropathic pruritus. Importantly, the Phox2a; tTA expression occurs in a spatially restricted population of skin keratinocytes that overlaps precisely with the skin area that is scratched. Localized G_i-DREADD-mediated inactivation of these Phox2a-keratinocytes completely reverses the skin lesions, while inducible tTA activation of keratinocytes initiates the condition. Notably, ablation of TRPV1-expressing primary afferent neurons also reduces scratching and skin lesions, but this occurs slowly, over a course of two months. In contrast denervation induced loss of all cutaneous input rapidly blocks scratching. These findings identify the cellular, molecular, and topographic basis of a robust and chronic sensory neuron–dependent and gabapentin-responsive neuropathic itch that is initiated by genetic factors within keratinocytes.

chronic itch | neuropathic itch | DREADDs | keratinocytes | TRPV1 sensory neurons

Significance

Chronic itch remains a clinical condition that is difficult to manage; treatment can improve, in part, by experimental insights using new animal models of chronic itch. Here, we describe a highly localized model of neuropathic itch in mice that is associated with profound and persistent scratching. The scratching is managed by gabapentin and completely blocked by the antipruritic agent, nalfurafine, but is unresponsive to morphine. Importantly, the itch-induced scratching in this model is experimentally controllable, in both space and time, facilitating analysis of the neural and epithelial cells that contribute.

Epidermal keratinocytes are integral to cutaneous somatosensation (1, 2), and their dysfunction can lead to chronic itch conditions, such as atopic dermatitis and psoriasis (3, 4). Various studies have identified keratinocyte-derived signals that can engage sensory neurons, eliciting the unpleasant sensation of itch and triggering persistent scratching (5–7). One notable example is TSLP, which stimulates a subset of TRPV1- and TRPA1-positive pruriceptors and triggers itch (8). Among other specific classes of pruriceptors, TRPV1-positive primary sensory neurons are key mediators of a chronic itch condition (9–12). Additionally, chronic itch persists through gabapentin-responsive central sensitization of dorsal horn pruriceptive circuits, resulting in prolonged and excessive scratching and alloknesis (heightened itch in response to normally non-itch-provoking stimuli) (13, 14).

In the course of our studies of awake-state dorsal horn projection neuron calcium imaging (15), we identified a transgenic mouse model that, at five weeks of age, manifests with intense, spontaneous scratching directed at the shoulder. The scratching increases over time and provokes highly localized scratching-induced skin lesions bilaterally. Here, we show that the scratching in this model is resistant to morphine, but effectively managed by the antipruritic kappa opioid receptor agonist, nalfurafine (16), and gabapentin, indicating that these mice manifest a neuropathic itch condition. Additionally, we demonstrate the necessity and sufficiency of localized keratinocyte activity for this condition. We establish that cutaneous peripheral nerves are necessary to sustain the scratching and demonstrate that TRPV1-positive primary sensory neurons are a key intermediary. This model of chronic itch underscores the significance of keratinocyte–peripheral nerve communication and details spatial and temporal determinants of its initiation and persistence.

Results

Development of Spontaneous Scratching and Focal Skin Lesions in Mice With Constitutive tTA-GCaMP6 Expression in the Phox2a Lineage. We crossed Phox2a-Cre mice with GCaMP6-expressing TIGRE 2.0 lines that, after Cre-lox recombination, express tTA2 (tTA), under the CAG promoter, and GCaMP6, under tTA control (Fig. 1*A*). Beginning at 5 wk of age, in Phox2a; tTA-GCaMP6 mice, we observed significant spontaneous scratching that increased in frequency over time (Fig. 1*B*). As the scratching progressed, prominent

Author affiliations: [a]Department Anatomy, University of California, San Francisco, CA 94158; [b]Department Dermatology, University of California, San Francisco, CA 94158; [c]Division Dermatology, San Francisco Veterans Affairs Healthcare System, San Francisco, CA 94121; [d]Neural Circuit Development Research Unit, Institut de Recherches Cliniques de Montréal, Montréal, QC H2W 1R7; and [e]Department Neurological Surgery, University of California, San Francisco, CA 94158

Author contributions: A.J.C., S.W.K., and A.I.B. designed research; A.J.C., S.W.K., M.E.J., H.L.C., E.M., M.R.C., V.D., S.R., R.C., and J.M.B. performed research; A.K. and R.C. contributed new reagents/analytic tools; A.J.C., S.W.K., and M.E.J. analyzed data; and A.J.C. and A.I.B. wrote the paper.

The authors declare no competing interest.

This article is a PNAS Direct Submission.

[1]A.J.C. and S.W.K. contributed equally to this work.

[2]To whom correspondence may be addressed. Email: allan.basbaum@ucsf.edu.

This article contains supporting information online at https://www.pnas.org/lookup/suppl/doi:10.1073/pnas.2411724122/-/DCSupplemental.

Published June 11, 2025.

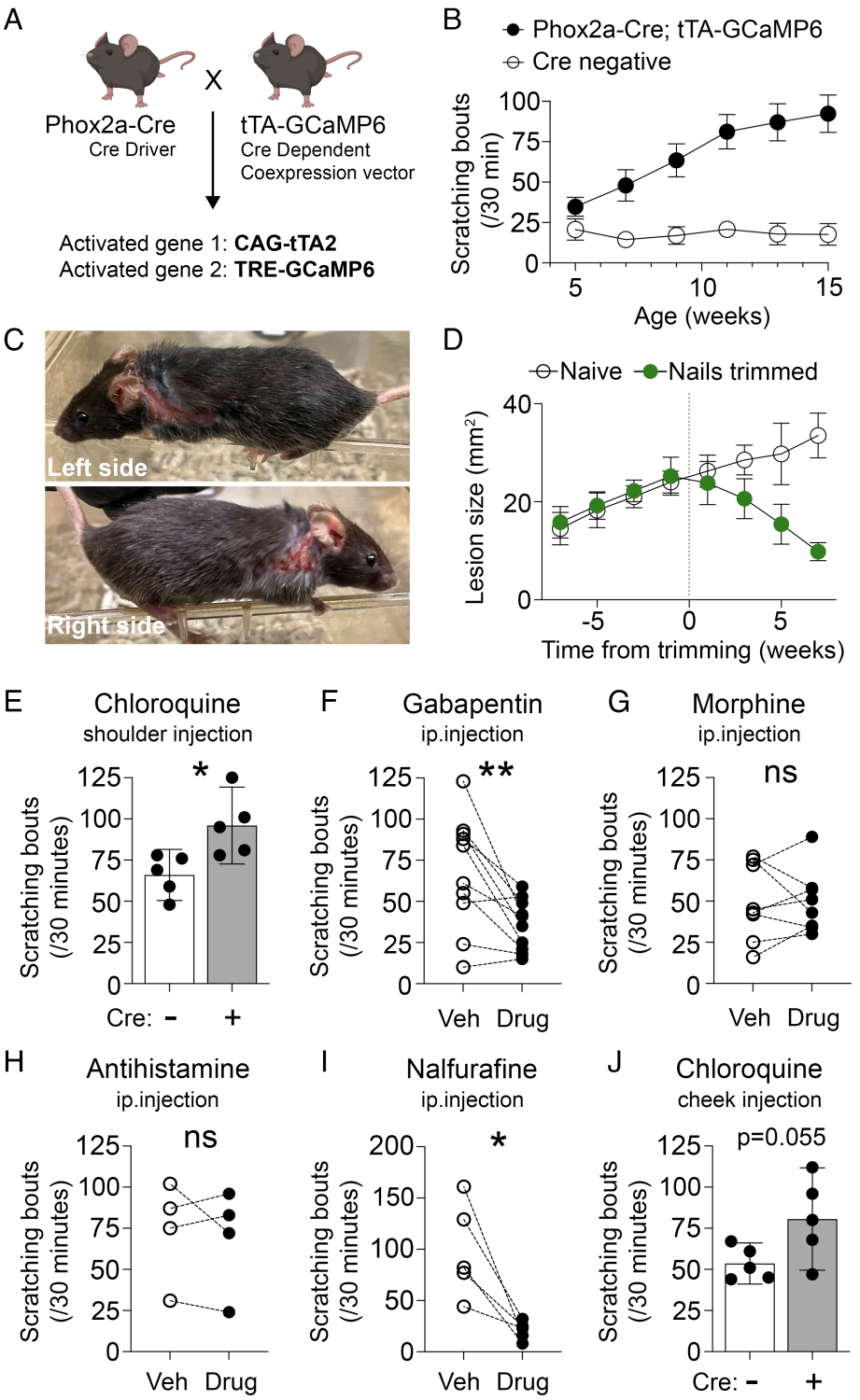

Fig. 1. Constitutive tTA-GCaMP6 transgene expression in the Phox2a+ lineage provokes a neuropathic itch condition. (*A*) Transgenic breeding scheme to express GCaMP6 in the Phox2a lineage, using Phox2a-Cre mice and TIGRE 2.0 reporter mice. TIGRE 2.0 mice, specifically of the Ai162 line, coexpress two genes, tTA2 and GCaMP6s, after Cre-mediated recombination. (*B*) Analysis of spontaneous scratching in Phox2a-Cre; tTA-GCaMP6 mice. Scratching becomes obvious at 5 wk of age and increases in frequency thereafter. Phox2a-Cre+; tTA-GCaMP6 (N = 13), Cre-; tTA-GCaMP6 (N = 15). GCaMP6s and 6f data are compiled in Fig. 1*B*; see *SI Appendix*, Fig. S2*A* for a direct comparison of the 6s vs. 6f GCaMP variants. (*C*) Representative images of bilateral, shoulder-localized erosive skin lesions in a 12 wk Phox2a; tTA-GCaMP6s mouse. (*D*) Weekly hind paw nail trimming reduces the size of skin lesions in Phox2a; tTA-GCaMP6 mice. Trimmed (N = 5), Untrimmed (N = 4). (*E*) Scratching provoked by intradermal injection of chloroquine at the shoulder in Phox2a-Cre+; tTA-GCaMP6 mice compared to Cre- littermate control mice. Data points represent individual mice. For (*F–I*), lines connect paired data points of the same mouse 24 h apart. Intraperitoneal injection of (*F*) Gabapentin 30 mg/kg and (*I*) Nalfurafine 20 μg/kg, compared to an injection of the drug vehicle, reduced scratching bouts in Phox2a-Cre; tTA-GCaMP6 mice. However, no difference in scratching bouts after ip. injection of (*G*) morphine 10 mg/kg or (*H*) cetirizine 30 mg/kg in Cre+ mice. (*J*) Scratching provoked by intradermal injection of chloroquine at the cheek in Cre+; tTA-GCaMP6 mice compared to Cre- littermate control mice. Data points represent individual mice. Statistics were analyzed by two-tailed unpaired (*E* and *J*) or paired (*F–I*) *t* test. Error bars indicate the 95% CI. **P* < 0.05, ***P* < 0.01, ns = nonsignificant.

erosive skin lesions developed bilaterally, localized to the dorsal shoulder areas (Fig. 1*C* and *SI Appendix*, Fig. S1*A*). Over time, the skin lesions at the dorsal shoulder increased in size, commonly extending to the abdomen. As nail trimming alleviated the lesions, we concluded that the erosive skin lesions were scratching-dependent (Fig. 1*D*). This phenotype was 100% penetrant, and homozygosity of the tTA-GCaMP6 allele in Phox2a-Cre mice accelerated the course of skin pathology (*SI Appendix*, Fig. S1*B*). Interestingly, although shoulder lesions consistently occurred in all animals, a subset of mice also developed erosion and erythema at the ear, suggesting variable effects at different anatomical locations. Sex did not change skin lesion presentation, and progressive scratching was observed in both male and female Phox2a; tTA-GCaMP6 mice (*SI Appendix*, Fig. S1*C*).

The Scratching Phenotype in the Phox2a; tTA-GCaMP6 Mice Is a Manifestation of a Neuropathic Itch Condition. As the scratching occurred in the absence of exogenous pruritogens, we hypothesized that the phenotype is a manifestation of profound sensitization that provoked spontaneous, itch-induced scratching in the Phox2a; tTA-GCaMP6 mice. To address this hypothesis, we first assessed pruritogen-evoked scratching by injecting the potent pruritogen, chloroquine, at the shoulder. In fact, the level of pruritogen-evoked scratching at the shoulder was significantly greater in Phox2a; tTA-GCaMP6 mice compared to their Cre-negative counterparts. We conclude that the spontaneous scratching did indeed result from a local skin sensitization (Fig. 1*E*).

To test whether the profound scratching arose from and is a manifestation of a neuropathic itch condition, we examined responsiveness to neuropathic itch pharmacotherapies. Gabapentin (ip. 30 mg/kg), a first-line neuropathic itch treatment (17), significantly reduced spontaneous scratching in the Phox2a; tTA-GCaMP6 mice (Fig. 1*F*). Interestingly, although pruritus is a common side effect of opiate administration, particularly after intrathecal injection (18), morphine (ip. 10 mg/kg) did not change scratching relative to the already heightened scratching in the Phox2a; tTA-GCaMP6 mice (Fig. 1*G*). That the scratching was not reduced by morphine also suggests that it was not driven by a peripheral inflammatory condition. Also, the itch was not histaminergic; the antihistamine Cetirizine (ip. 30 mg/kg) did not affect scratching frequency (Fig. 1*H*). We next tested nalfurafine (ip. 20 μg/kg), a highly selective agonist of κ-opioid receptors (KOR) and an effective antipruritic in humans with uremic pruritus (19, 20). Fig. 1*I* shows that nalfurafine significantly reduced scratching in Phox2a; tTA-GCaMP6 mice, effectively arresting the behavior, consistent with our hypothesis that a neuropathic itch had developed.

Interestingly, although spontaneous scratching of the cheek was not observed, chloroquine injection into the cheek did increase evoked scratching compared to littermate controls (Fig. 1*J*). This suggests that a generalized sensitization has occurred in these mice, but that it predominates in the shoulder. We also tested an alternative hypothesis, namely that these mice have a generalized sensitization of neural circuits that would influence both itch and pain processing. In fact, measures of acute pain processing did not differ between Phox2a; tTA-GCaMP6 mice and their littermate Cre negative controls. Specifically, we found no differences in withdrawal-based thermal (heat or cold) or mechanical sensitivity assays, or pain-associated wiping behaviors after intradermal algogen cheek injection with capsaicin (*SI Appendix*, Fig. S1 *D–G*). These negative findings are consistent with other preclinical chronic itch models, such as Bhlhb5 mutant mice, which have excessive scratching, but no change in acute nociception (21). Furthermore, as noted above, an intraperitoneal injection of morphine, at a dose that can reverse tissue injury-induced heat hypersensitivity, did not reduce the frequency of scratching (Fig. 1*G*). Based on the sensitization to the pruritogen, chloroquine, and the antipruritic effectiveness of nalfurafine and gabapentin, we conclude that the phenotype is indeed a manifestation of a profound neuropathic itch condition.

The Neuropathic Itch Phenotype Is Genetically Dependent on tTA, not GCaMP6. We next examined the genetic basis for this neuropathic itch presentation in the Phox2a; tTA-GCaMP6 mice. We compared three related Cre-dependent reporter lines that varied the configuration of tTA and GCaMP6 within the transgenic vector (Fig. 2*A*), keeping their combination with Phox2a-Cre consistent. We first established that adult Phox2a-Cre crossed to the Ai96 line, which lacks tTA but contains CAG-driven GCaMP6s, did not develop spontaneous scratching or scratching-induced lesions (Fig. 2*B*, cyan circles). Next, we compared a slow and fast kinetic variant of GCaMP6, which were cloned into the same Cre-dependent tTA cassette, namely Ai162 (GCaMP6s) vs. Ai148 (GCaMP6f). As both the Ai162 and Ai148 presented with similar skin lesions, we conclude that subtle changes in calcium binding kinetics of GCaMP6 are not a significant determinant of the progressive itch phenotype (Fig. 2*B*, purple vs. pink circles, also see *SI Appendix*, Fig. S2*A*). Importantly, the Cre-dependent tdTomato reporter line (loxp-STOP-loxp-CAG-tdTomato), Ai9, which was the primary readout for our subsequent fate mapping studies, did not elicit scratching when crossed to Phox2a-Cre mice (Fig. 2*B*, orange circles) and did not change Phox2a; tTA-GCaMP6 scratching levels (Figs. 2*B*, blue circles). We histologically confirmed that cytoplasmic GCaMP6 fluorescence was visible in spinal cord tdTomato-marked neurons in each of these reporter lines (Ai96, Ai148, and Ai162 crossed to Phox2a-Cre and Ai9) (*SI Appendix*, Fig. S2 *B* and *C*). Based on these observations, we conclude that a genetic configuration that includes tTA is necessary for the neuropathic itch phenotype.

We also bred Phox2a-Cre to another tTA-driven reporter line, which shares the same tTA2 configuration as Ai162 and Ai148, but does not contain GCaMP6 (Fig. 2*C*). In TIGRE-MORF-GFP (Ai166) mice (22), all cells expressing Cre undergo recombination and express tTA. However, due to a stochastic translational switch within the MORF sequence upstream of the GFP gene only 1 to 2% of Cre+ cells permit tTA-driven GFP expression. Histological examination of these mice confirmed the expected sparse GFP expression pattern, and confirmed tTA activity in spinal Phox2a-Cre neurons (Fig. 2*D*). Although the Phox2a-Cre; Ai166 combination frequently resulted in perinatal lethality, we found that this could be prevented through embryonic doxycycline administration, which directly inhibits tTA activity (*SI Appendix*, Fig. S2 *D–E*). Notably, the few adult Phox2a; Ai166 mice that were viable without doxycycline treatment developed spontaneous scratching directed at the shoulders and bilateral skin lesions (Fig. 2*E* and *SI Appendix*, Fig. S2*F*). Collectively, these findings demonstrate that tTA alone, independent of GCaMP6, is both necessary and sufficient to produce the highly localized features of the Phox2a; tTA-GCaMP6 phenotype.

The Neuropathic Itch Phenotype Is Dependent on tTA Activity. Taking advantage of the built-in ability for the Tet system to be exogenously controlled, we next functionally tested the requirement of tTA activity for the incidence of spontaneous scratching in Phox2a; tTA-GCaMP6 mice. First, by administering doxycycline (Dox) through the chow (200 mg/kg in diet), we chronically inhibited

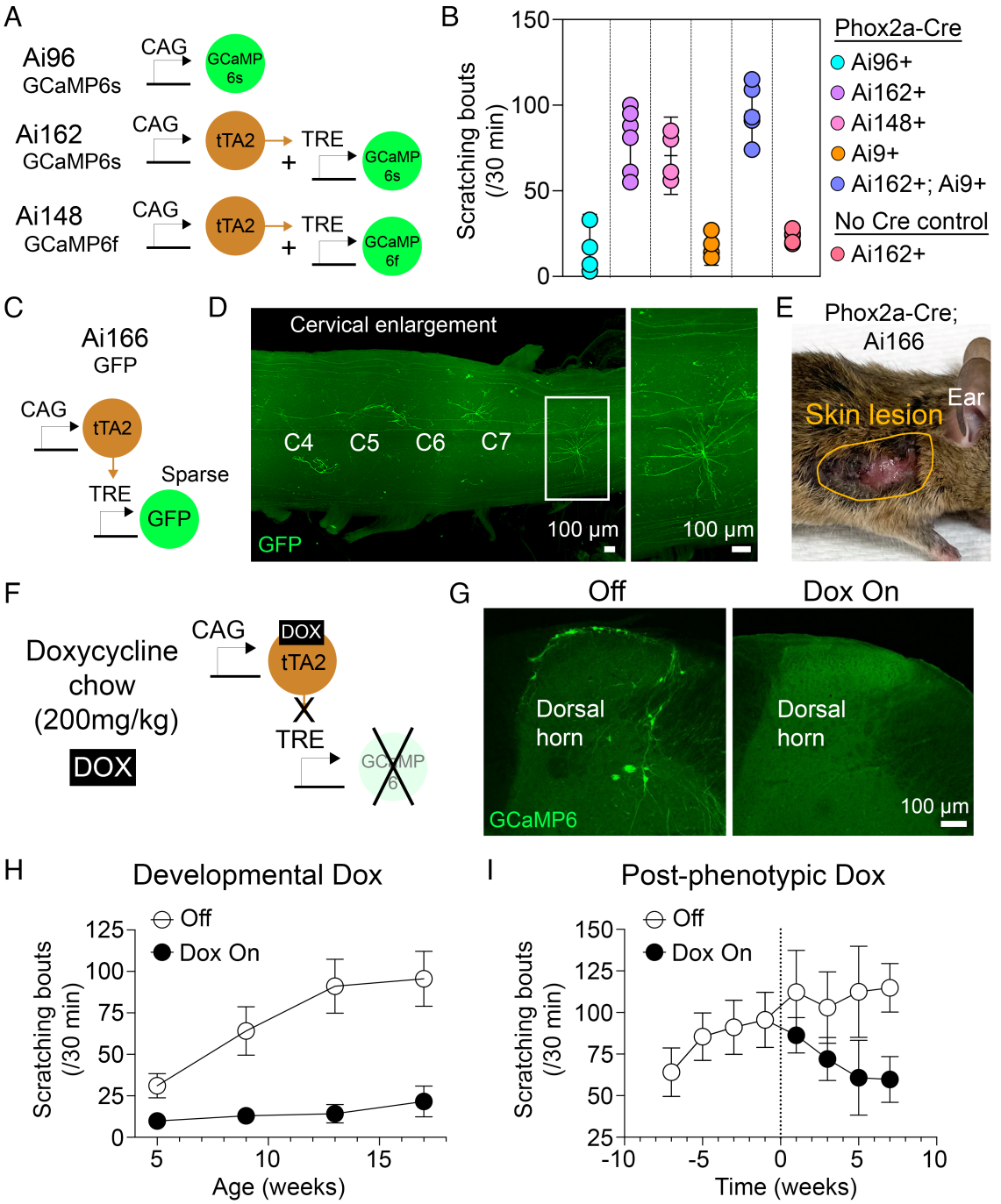

Fig. 2. tTA independently controls the scratching phenotype in Phox2a; tTA-GCaMP6 mice. (*A*) The genetic configuration of the Ai96 (GCaMP6s) line, without tTA transcriptional control, compared to two tTA-driven lines: Ai162 (GCaMP6s) and Ai148 (GCaMP6f). (*B*) Comparison of spontaneous scratching frequency at 11 wk of age across the indicated genotypes crossed with Phox2a-Cre or control mice without Cre. Colored dots represent individual mice. Ai9 = Cre-dependent CAG-tdTomato reporter used for fate mapping studies. (*C*) The genetic configuration of Ai166 is the same as Ai162 except that, instead of GCaMP6, it encodes GFP which is expressed in a random subset of Cre+ cells. (*D*) A maximum intensity projection image of a SHIELD-cleared, whole-mount spinal cord from a Phox2a-Cre; Ai166 mouse shows sparse, cellular GFP expression. Specifically, the cleared cervical enlargement is shown, and cervical spinal segments are annotated as (C4–C7). Inset provides a magnified image of a single GFP neuron. (*E*) Image of a Phox2a-Cre; Ai166 mouse showing a localized skin lesion phenotype similar in location to Phox2a; Ai162 mice. (*F*) Doxycycline 200 mg/kg, administered through the chow, inhibits tTA activity through direct binding, arresting its transcriptional activity. (*G*) Spinal cord histology confirms the downregulation of GCaMP6s in dorsal horn projection neurons of mice on Doxycycline chow. (*H*) Doxycycline chow provided during pregnancy and after weaning prevents the development of scratching. Dox diet "On" (N = 5), Standard diet "Off" (N = 9). (*I*) Doxycycline started in adulthood partially reduces spontaneous scratching. Dox On (N = 4), Dox Off (N = 5). Error bars indicate the 95% CI.

tTA activity, which repressed GCaMP6 transcription (Fig. 2*F*). As predicted, Dox-treated adult mice downregulated the GCaMP6 protein in Phox2a dorsal horn projection neurons (Fig. 2*G*).

Initially, we administered Dox chow throughout the development of the Phox2a; tTA-GCaMP6 mice, including in utero, by its ad libitum Dox feeding to the pregnant dams (*SI Appendix*, Fig. S2*D*). Strikingly, developmental Dox exposure fully prevented the development of spontaneous scratching and skin lesions (Fig. 2*H*). Furthermore, and unexpectedly, when switched off Dox chow as adults, these developmental Dox-treated mice did not develop the characteristic scratching-induced lesions, throughout the rest of their lifespan. On the other hand, consistent with an ongoing effect of tTA in promoting a neuropathic itch, Dox feeding to symptomatic adults significantly reduced scratching

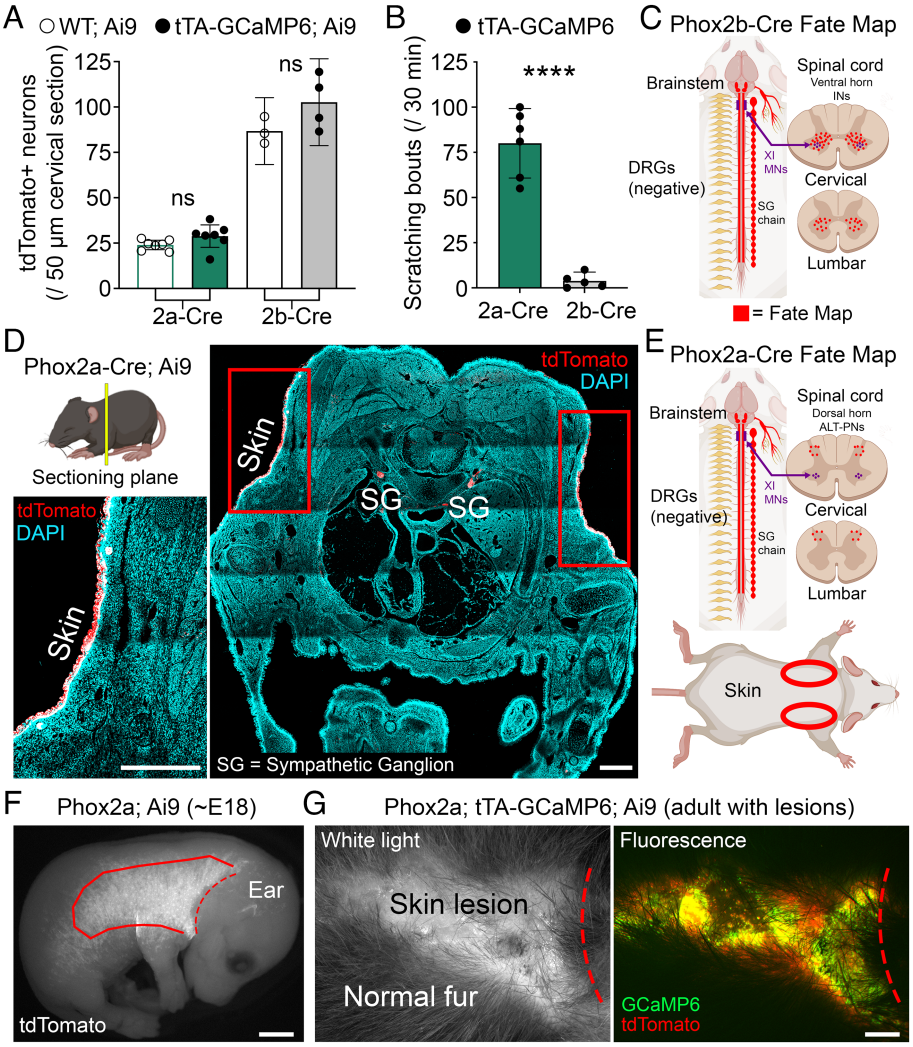

Fig. 3. Fate mapping identifies keratinocytes within the Phox2a lineage as the topographical determinant of scratching. (*A*) Quantification showing comparable numbers of tTA+ and tTA− ("wild-type") neurons in the cervical spinal cord for both Phox2a-Cre and Phox2b-Cre lines. Ai9 = Cre-dependent CAG-tdTomato reporter used to visualize neurons. (*B*) Phox2b-Cre; tTA-GCaMP6 mice do not exhibit the scratching phenotype observed in Phox2a-Cre; tTA-GCaMP6 mice. (*C*) Schematic of the Phox2b-Cre fate map (annotated in red) in the nervous system based on Cre-dependent reporter expression. Phox2b-Cre labels many of the same populations of neurons as Phox2a-Cre (compare to *E*). Purple color specifically annotates the XI motoneurons. (*D*) Whole-body cross-section histology of a 7-d-old Phox2a-Cre; Ai9 mouse reveals tdTomato reporter expression in the skin surrounding the shoulder but not in deeper soft tissues, except the sympathetic ganglia (SG). Red boxes define the boundary of the skin where reporter expression is observed, which is bilateral. The left box outlines the *Left* inset image. (*E*) The Phox2a-Cre lineage includes both neuronal populations and skin keratinocytes (approximate expression boundary in the skin is indicated by red ovals). (*F*) Visualized by tdTomato pseudocolored in white, a Phox2a; Ai9 embryo reveals a striking topography of reporter expression outlined in red. The red dotted line defines the boundary of Cre-mediated recombination at the neck. (*G*) Monochrome image showing a hairless skin lesion in an adult Phox2a-Cre; Ai9; Ai162 mouse (*Left*). Fluorescent imaging reveals GCaMP6s (green) and tdTomato (red) signals throughout the lesioned area but not in the surrounding skin (*Right*). The red dotted line indicates the neck boundary of recombination. (Scale bar, 500 µm.) Statistics were analyzed using two-tailed unpaired *t* test. Error bars represent 95% CI. ****$P < 0.0001$, ns = nonsignificant.

(Fig. 2*I*). We conclude that in the Phox2a lineage, unrestricted tTA activity is essential for inducing the neuropathic itch phenotype and for sustaining the resulting skin pathology.

Despite tTA Expression, Phox2a Neurons Develop Normally. We next examined the anatomical basis for this remarkably localized neuropathic itch presentation in the Phox2a; tTA-GCaMP6 mice. As Phox2 (2a and 2b) genes are purportedly neural-specific and because of the restricted topography of the scratching, which was directed to cervical dermatomes, we hypothesized that tTA expression selectively perturbed cervical Phox2a neuronal development. First, by counting the number of cervical tdTomato+ neurons in mice with and without tTA-GCAMP6, we investigated a possible dysfunction in neurogenesis or survival of Phox2a-expressing neurons. In fact, Fig. 3*A* shows that the number of tdTomato+ neurons (Phox2a-Cre; LSL-tdTomato) in the cervical spinal cord did not differ from the number of tdTomato+ neurons in mice expressing tTA-GCaMP6 (Phox2a-Cre; LSL-tdTomato; tTA-GCaMP6). We also crossed tTA-GCaMP6 mice with Phox2b-Cre mice. Phox2b is a paralogous gene of Phox2a, which is coexpressed in many, but not all, neuronal lineages with Phox2a (23). Despite a threefold increase in the number of tdTomato+ cervical spinal cord neurons in the Phox2b-Cre; LSL-tdTomato mice, we did not detect a difference in neuronal number across tTA-GCaMP6 genotypes. We conclude that tTA expression in these Phox2 Cre lines is not disruptive to neurogenesis, nor is it neurotoxic.

Next, we surveyed the morphology of fate-mapped cervical spinal neurons for abnormalities. In control Phox2a-Cre; LSL-tdTomato mice, we observed tdTomato+ neurons, as expected, in

dorsal horn laminae I and V (*SI Appendix*, Fig. S3*A*). Similarly, in Phox2a-Cre; LSL-tdTomato; tTA-GCaMP6 mice, laminae I and V tdTomato+ neurons were readily identifiable (*SI Appendix*, Fig. S3*B*) and exhibited fusiform and multipolar morphologies, consistent with previous reports (24, 25). Furthermore, the XIth cranial motoneurons and their efferents that form the XIth cranial nerve were similarly observed in both genotypes, with and without tTA-GCaMP6 (*SI Appendix*, Fig. S3 *A* and *B*). The XIth cranial nerve was also visible in Phox2b-Cre; LSL-tdTomato mice and appeared similarly with and without tTA-GCaMP6 (*SI Appendix*, Fig. S3 *C* and *D*). We conclude that important developmental processes of neurogenesis, fate specification, migration, and axonal pathfinding are largely uninterrupted by constitutive tTA expression in Phox2a-Cre and Phox2b-Cre mice.

tTA Expression in Phox2b Neuronal Populations does not Provoke Scratching. Importantly, in contrast to what was observed in the Phox2a-Cre mice, Phox2b-Cre mice crossed to tTA-GCaMP6 did not spontaneously scratch as adults or exhibit skin lesions (Fig. 3*B*). This result allowed us to compare the fate maps, using Cre-dependent tdTomato reporter expression, of Phox2a-Cre and Phox2b-Cre lines and identify the neural populations present in both lineages, which could point to those unlikely to underlie the neuropathic itch condition. The most striking difference was that Phox2a-Cre, but not Phox2b-Cre, selectively labeled dorsal horn projection neurons, which have been implicated in other mouse models of chronic itch (20, 26, 27). Importantly, however, a shared fate map included several neural populations that either received or transmitted signals to cervical dermatomes. Specifically, accessory nerve motoneurons (XI) located in the cervical enlargement mentioned above and cervical sympathetic postganglionic neurons were fate-mapped in both lines (Fig. 3 *C* vs. *E*). Shared fate maps were also found in the brain (*SI Appendix*, Fig. S3*E*). We conclude from these studies that tTA activation in these common neural populations does not correlate with and likely does not initiate the scratching phenotype. In support of this conclusion, chemically induced sympathectomy in Phox2a; tTA-GCaMP6 mice did not influence scratching (*SI Appendix*, Fig. S3*F*). Last, as an alteration in peripheral sensory neuron function could contribute to a localized scratching phenotype, it is significant that in the Phox2a-Cre mice we observed little to no reporter expression in dorsal root ganglion (DRG) neurons (cervical or otherwise) (*SI Appendix*, Fig. S3*G*).

The Phox2a-Cre, but not the Phox2b-Cre-Generated Fate Map, Includes Skin Keratinocytes. Focusing outside the nervous system, we expanded our fate map screening for reporter expression to the localized distribution of the scratching and skin lesions. To screen for reporter expression, we performed whole-body cross-section histology of 7-d-old Phox2a; LSL-tdTomato mice, which revealed tdTomato fluorescence limited to the epidermis around the dorsal shoulder, never extending to the underlying dermis or muscle (Fig. 3*D*). Based on localization in all layers of the epidermis, including the hair follicle, we determined that these epidermal cells in the Phox2a-Cre lineage are keratinocytes. Additionally, in Phox2a-Cre mice, we recorded skin tdTomato reporter expression in late gestation embryos and adults, but not in the Phox2b-Cre; LSL-tdTomato mice of comparable age (*SI Appendix*, Fig. S3 *H* and *I*). In the Phox2a-Cre; LSL-tdTomato mice, cutaneous tdTomato expression was located predominantly at the shoulder, some at the tip of the ear, but none in the face (*SI Appendix*, Fig. S3*J*).

Strikingly, the shoulder-restricted topography of the tdTomato reporter expression, which is clearly seen in the Phox2a; LSL-tdTomato embryos (Fig. 3*F*), mirrors the topography of skin lesions that we recorded in the Phox2a; tTA-GCaMP6 adults (Fig. 3*G*). In adult mice with lesions, whole-mount imaging and cross-sectional histology of lesioned skin revealed robust in situ GCaMP6 and tdTomato fluorescence limited to the lesional area (*SI Appendix*, Fig. S4 *A* and *B*). GCaMP6 fluorescence observed in skin lesions was much higher than the background autofluorescence detected in scratch-induced lesions of transgenic mice that overexpress IL-31 without GCaMP6 (24) (*SI Appendix*, Fig. S4 *C* and *D*). Additionally, skin samples from both Cre-negative control mice and Phox2a; tTA-GCaMP6 mice maintained on doxycycline exhibited minimal fluorescence (*SI Appendix*, Fig. S4 *E* and *F*).

Consistent with our observation that erosion and erythema of the ear developed in some Phox2a; tTA-GCaMP6 mice, we detected a small population of GCaMP6 and tdTomato reporter-labeled cells at the ear tip (*SI Appendix*, Fig. S4*G*). However, most Phox2a; tTA-GCaMP6 mice with significant shoulder lesions did not develop ear lesions (*SI Appendix*, Fig. S4*H*). This suggests that while tTA activation within this limited ear population may sensitize the skin locally, it typically fails to reach the threshold required to induce persistent scratching and lesions. Thus, we hypothesize that tTA activation in a large, confluent population of keratinocytes that form the shoulder skin is likely the primary driver of the scratching phenotype.

Keratinocyte-Selective tTA Expression Is Sufficient to Produce Skin Lesions in KRT14-CreER; tTA-GCaMP6 Mice. To test whether tTA activation in keratinocytes is indeed sufficient to induce the scratching phenotype, we initiated studies with the Keratin14 (KRT14)-CreER mice (28). In these mice, to activate CreER in keratinocytes, we unilaterally applied 4-hydroxytamoxifen (4-OHT) to the depilated skin around the shoulder and ear (Fig. 4*A*). One month after the 4-OHT application, we verified the expression of tdTomato and GCaMP6 in the shoulder skin of KRT14-CreER; LSL-tdTomato; tTA-GCaMP6 mice (Fig. 4*B*). As tdTomato and GCaMP6 expression were found primarily in areas that also showed hair loss, which is typically seen before a lesion develops, we are confident that the area of Cre-mediated recombination was limited to where we applied topical 4-OHT. Importantly, we also compared experimental conditions within individual mice, by topical exposure of 4-OHT to one side of the body and vehicle to the other side. Strikingly, but only at a remarkable delay of 2 to 3 mo, skin lesions developed only on the side exposed to 4-OHT (Fig. 4 *C*–*E*). These skin lesions included the shoulder and ear, which were topographically mirrored by GCaMP6 expression (*SI Appendix*, Fig. S5*A*).

We also used a systemic strategy to activate tTA-GCaMP6 selectively in keratinocytes throughout the body. Tamoxifen injected intraperitoneally in adult KRT14-CreER; tTA-GCaMP6 mice led to a development of spontaneous scratching and skin lesions, with scratching becoming obvious at 1 mo and lesions becoming obvious by 2 mo (*SI Appendix*, Fig. S6 *A*–*C*). Curiously, in contrast to Phox2a-Cre activation, in which lesions are localized to the shoulder, systemic KRT14-CreER activation provoked intense scratching-induced skin lesions at the ventral neck (*SI Appendix*, Fig. S6*D*). In a second cohort of systemically activated KRT14-CreER; tTA-GCaMP6 mice, we confirmed the characteristic ventral neck lesions and upon closer examination also observed small ear lesions (*SI Appendix*, Fig. S6*E*). This finding suggests that itch is triggered at multiple sites in these mice, as would be expected from a systemic manipulation. Importantly,

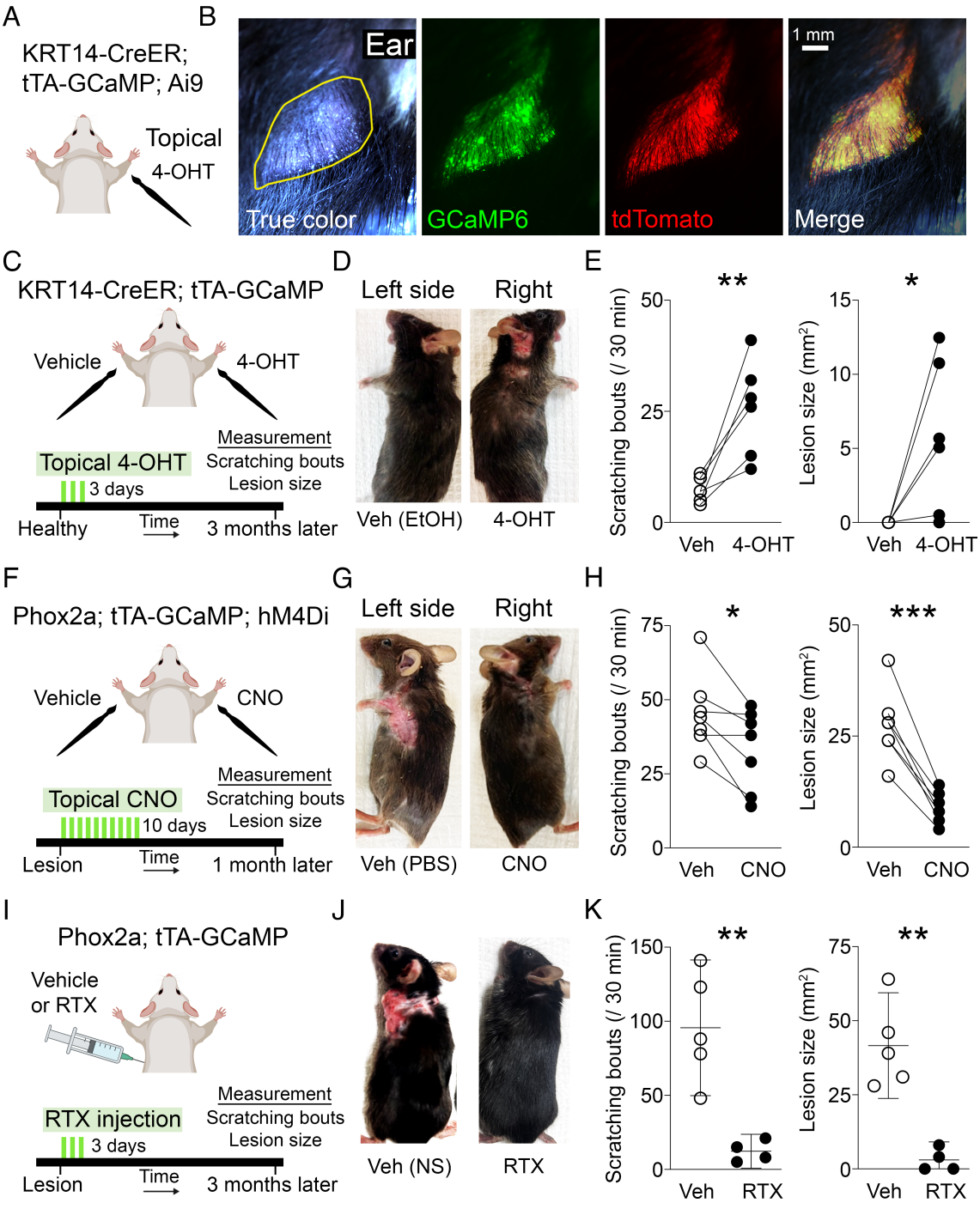

Fig. 4. Skin pathology can be controlled by the selective manipulation of keratinocytes or by the ablation of TRPV1 sensory neurons. (*A* and *B*) Unilateral 4-OHT application to the skin and validation of GCaMP6 and tdTomato reporter expression at one month after treatment. A hairless area (outlined in yellow) is typical of prodromal lesion sites. (*C*–*K*) Three experiments are detailed horizontally, one experiment per row. (*C*, *F*, and *I*) Experimental scheme and timeline. (*D*, *G*, and *J*) Example images of the three differing treatments after measurement. (*E*, *H*, and *K*) Scratching and skin lesion analysis of each experiment. Connected lines in (*E* and *H*) are measurements from either the *Left* or *Right* side of an individual animal. As RTX-mediated ablation is irreversible, the experiment in (*I*–*K*) was compared across groups of mice. Accordingly, statistics were analyzed by two-tailed paired (*E* and *H*) or unpaired (*K*) *t* test. $^{*}P < 0.05$, $^{**}P < 0.01$, $^{***}P < 0.001$.

despite keratinocyte-selective tTA activation throughout the body, testing of the hindpaw did not reveal a mechanical or thermal hypersensitivity (*SI Appendix*, Fig. S6 *F* and *G*), which rules out a generalized hypersensitivity of primary sensory and spinal cord circuits.

Importantly, as expected from the particular Cre line used, we verified that GCaMP6 was not expressed in the spinal cord of systemically activated KRT14-CreER; tTA-GCaMP6 mice (*SI Appendix*, Fig. S7*A*) but was robustly expressed in the ventral neck skin lesions (*SI Appendix*, Fig. S7*B*). The absence of GCaMP6 expression at the ventral neck skin of Phox2a-Cre; tTA-GCaMP6 mice, which do not develop skin lesions of the ventral neck, strongly supports the functional relationship between tTA-GCaMP6 skin expression and skin pathology (*SI Appendix*, Fig. S7*C*).

To investigate how tTA expression in keratinocytes triggers itch, we analyzed four genes recently linked to itch initiation through keratinocyte–sensory neuron signaling. In skin samples from KRT14-CreER; tTA-GCaMP6 mice, 2 mo after Tamoxifen administration, compared to skin from Tamoxifen-injected control littermates without Cre, we measured expression levels of

TSLP (8), IL33 (29), POSTN (7), and EDN1 (30) by qPCR. Our analysis revealed that skin with tTA-GCaMP6 activation showed increased expression of TSLP, IL-33, and Periostin; Endothelin-1 levels did not change (*SI Appendix*, Fig S8). We conclude that tTA stimulates keratinocytes to release a set of itch-associated factors that activate cutaneous pruriceptors and downstream pruritogenic circuits in the dorsal horn.

Regional Keratinocyte-Selective tTA Activation Induces Localized Itch and Correlated Dorsal Horn Neuronal Activation. In both Phox2a-Cre mice and our KRT14-CreER experiments, we observed a clear spatial correlation between tTA-GCaMP6 activation in the skin and scratching. Activation of KRT14-CreER, by unilateral topical application of tamoxifen to the shoulder and ear, consistently produced unilateral scratching and skin lesions of the shoulder and ear in these mice. This spatial pattern had a functional correlate in the cervical dorsal horn of the spinal cord, namely ipsilateral upregulation of neuronal phospho-ERK1/2 (pERK) immunoreactivity (*SI Appendix*, Fig. S5*B*).

Interestingly, in systemically activated KRT14-CreER; tTA-GCaMP6 mice, we observed a different pattern of behavior that evolved over time. At 1 mo post-Tamoxifen injection, spontaneous scratching occurred diffusely across the body (*SI Appendix*, Fig. S9 and Movie S1). However, by 2 mo, as significant focal lesions developed at the ventral neck, scratching predominated at this specific location. This behavioral progression was paralleled by a broader, bilateral pattern of dorsal horn activation, in contrast to control mice that had minimal pERK expression (*SI Appendix*, Fig. S7 *B* vs. *D*).

Additionally, the severity of the phenotype scaled with the degree of tTA activation during development. The most compelling evidence came from our experiments using Hoxb8-FLPo mice crossed with FLP-dependent CAG-tTA2 reporter mice (Ai195 line). When we activated tTA in all tissues caudal to C7 (31), we observed particularly severe outcomes: widespread skin dysplasia concentrated in the groin area, accompanied by stereotyped licking and biting behaviors specifically targeting this region (*SI Appendix*, Fig. S9). Collectively, these experiments (Phox2a-Cre, KRT14-CreER, and Hoxb8-FLPo) underscore the topographical relationship between tTA expression and the resulting itch phenotype.

Keratinocyte Signaling Is Necessary for the Maintenance of Spontaneous Scratching and Skin Lesions in Phox2a; tTA-GCaMP6 Micebs. To test whether keratinocyte activity not only triggers, but also maintains the scratching phenotype in Phox2a; tTA-GCaMP6 mice, we created a triple transgenic line in which the Phox2a-expressing keratinocytes also express a Cre-dependent hM4Di inhibitory DREADD (Fig. 4*F*). To restrict DREADD-mediated inhibition to the keratinocytes, we applied the DREADD agonist CNO topically and unilaterally on adult mice with significant scratching-induced lesions. Phosphate-buffered saline (PBS) was topically applied to the contralateral lesion as a control. This topical application was repeated daily for 10 d. Fig. 4 *G* and *H* demonstrate that 20 d after discontinuing topical CNO application, Phox2a; tTA-GCaMP6; LSL-hM4Di mice exhibited a significant reduction in scratching bouts and a marked decrease in the size of skin lesions. Notably, these effects were observed only on the CNO applied side.

TRPV1-Expressing Primary Sensory Neurons Sustain the Keratinocyte-Driven Neuropathic Itch Condition. Last, we investigated which sensory neurons are responsible for the keratinocyte-initiated itch in this model. As the majority of pruritogens provoke scratching by activating TRPV1-expressing afferents (32), we ablated TRPV1-expressing sensory neurons with the capsaicin superagonist resiniferatoxin (RTX) (33). We tracked scratching and lesion size after RTX injection and compared the results to littermate controls that received a vehicle injection (Fig. 4*I*). Consistent with the successful ablation of the TRPV1 population, the RTX-injected mice demonstrated significantly increased tail-flick response latency to noxious heat compared to controls (*SI Appendix*, Fig. S6*H*). And Fig. 4 *J* and *K* show that spontaneous scratching and skin lesions in RTX-injected Phox2a; tTA-GCaMP6 mice were arrested entirely. Remarkably, however, resolution of the scratching and skin lesions only occurred after a significant delay, almost 3 mo after RTX injection. This delayed resolution suggests that non-TRPV1 sensory neurons sustain the scratching phenotype.

As a further test of the dependence of the scratching phenotype on peripheral input, in Phox2a; tTA-GCaMP6 mice that exhibited significant bilateral spontaneous scratching, we performed unilateral cutaneous denervation. Strikingly, by 4 d after unilateral denervation, the mice stopped scratching the ipsilateral side and only scratched the contralateral, nerve-intact side (*SI Appendix*, Fig. S10), demonstrating the essential role of peripheral sensory input in maintaining itch.

Discussion

Here, we describe a chronic neuropathic itch model that develops spontaneously in Cre-lox-based double-transgenic mice, one that is characterized by a remarkably confined distribution of scratching and consequent skin lesions. This focal disorder stems primarily from the selectivity of the Phox2a-Cre lineage, where activation of shoulder keratinocytes specifically triggers scratching at their location. Importantly, increasing Gαi signaling in Phox2a-keratinocytes, using topical DREADD-based methods, completely reversed the localized skin lesions and reduced scratching. Furthermore, as resiniferatoxin, gabapentin, and nalfurafine, but not the mu-opioid receptor agonist, morphine, alleviated the scratching, we conclude that TRPV1-expressing primary afferent neurons and kappa receptor-based pruritoceptive dorsal horn circuitry downstream of the keratinocytes are necessary contributors to the development of the neuropathic itch phenotype in this model.

Importantly, the predictive validity of this nalfurafine and gabapentin-sensitive model is comparable to other murine preclinical itch models. We also establish that this condition is non-histaminergic and is consistent with multiple studies demonstrating that keratinocyte released factors, namely, TSLP, IL-33, and Periostin, drive sensory neuron activity and trigger itch (7, 8, 29). The inducible and reversible nature of our approach offers unique flexibility for studying nonhistaminergic pruritic disorders, in which an initial trigger leads to sustained peripheral and central neural adaptations. Additionally, the ability to trigger itch topographically using KRT14-CreER mice may emulate site-specific dermatological conditions, such as psoriasis. In fact, the spatiotemporal effects of doxycycline provide advantages that complement cell-type-specific ablation or loss-of-function studies that are investigating the complex interplay between skin, immune responses, and neural components in the itch-scratch cycle (34). These experimental advantages enable a range of experiments, for example, investigating the contextual and topographical factors that influence keratinocytes to trigger itch rather than pain (2, 35, 36). In fact, in this model, tTA activation can be tested in both glabrous and hairy skin compartments, allowing comparisons of the resulting behaviors.

In neuropathic pain models, there is considerable evidence that sensitization of spinal dorsal horn neurons develops after an experimentally induced nerve or tissue injury and contributes to the chronic hyperalgesia/allodynia (37). Neuropathic itch mechanisms are also thought to involve a central sensitization mechanism, one that underlies chronic hyperknesis/alloknesis, but one that is less understood (13, 38). Based on several findings in the present study, we suggest that central sensitization of pruritoceptive neural circuits can sustain the tTA-induced scratching phenotype for months. In fact, functional and molecular correlates of central sensitization are present, namely a scratching phenotype that progressively increases in degree, duration, and spatial extent, along with a marked increase in phospho-ERK in the superficial layers of the dorsal horn. The efficacy of gabapentin also supports this hypothesis. Specifically, gabapentin counteracts the sensitization of spinal dorsal horn neurons, correlating with gabapentin's pronounced effects in reducing behavioral hypersensitivity in acute and chronic pain conditions (39). Additionally, the RTX experiment provides particularly compelling evidence that primary afferent-triggered central sensitization contributes to the persistence of the scratching. Only after a significant three-month delay did TRPV1 primary sensory neuron ablation fully reverse the skin lesion and scratching phenotype. We hypothesize that the keratinocytes not only communicate with TRPV1-expressing afferents to drive the neuropathic itch phenotype, but that there is also a concurrent activation of a non-TRPV1 population that interacts with sensitized dorsal horn pruritoceptive circuits (40).

In light of multiple reports of GCaMP toxicity in neurons, mostly with viral approaches, but also with transgenic mice (41, 42), it is significant that the molecular etiology of the scratching phenotype was not related to GCaMP6-associated toxicity. For example, tonic-clonic seizures associated with cell-type selective GCaMP6s expression, but not GCaMP6f, occur in the hippocampus (43). However, here we found that neither the selection of a slow nor a fast GCaMP6 variant significantly impacted the scratching phenotype. Furthermore, typical GCaMP toxicity signatures, such as ectopic nuclear localization associated with neuronal dysfunction, were not observed (44). Also, our finding that Phox2a-Cre; Ai166 (tTA-GFP) mice frequently exhibited perinatal lethality suggests a nuanced conclusion, namely that the GCaMP6 element of Ai162/148 lines actually prevents lethality rather than contributing to the phenotype. Thus, we conclude that expression of the CAG-driven tTA allele, not GCaMP6 or a related toxicity, is the determining factor for pathology.

Finally, we provide evidence that Gαi-mediated signaling rapidly resolves scratching-induced skin lesions. Although second messenger cascades in keratinocytes share similarities, they also have distinct properties. Gαs is associated with epithelial stem cell growth and maintenance, whereas Gαi signaling promotes proliferation (45). Previous studies have shown that activating Gαi signaling in keratinocyte cell lines and mice, specifically using the K5-Cre; LSL-hM4Di mice with systemic CNO treatment, leads to proliferation and prevents differentiation of keratinocytes (46). Additionally, the Gαi-coupled GPCR HCAR3 modulates keratinocyte growth in human keratinocytes by engaging Gαi signaling rather than β-arrestins (47). In conclusion, our results demonstrate that dysregulation of keratinocytes triggers pruriceptive neural pathways that culminate in a profound neuropathic itch phenotype. Most importantly, our findings introduce a potentially clinically applicable approach to completely reverse chronic itch through a gene therapy manipulation that permits topical activation of Gαi signaling in keratinocytes.

Materials and Methods

Transgenic Mouse Breeding and Maintenance. Animal procedures were conducted in accordance with the Guide for the Care and Use of Laboratory Animals, with the approval of the Institutional Animal Care and Use Committee at UCSF, in facilities accredited by the Association for the Assessment and Accreditation of Laboratory Animal Care International (AAALAC). UCSF LARC technicians provided animal husbandry and care. Phox2a-Cre mice (Roome et al. 2020) were backcrossed with C57BL/6 J mice for >5 generations. Ai162 (JAX #:031562), Ai96 (JAX #:028866), Ai148 (JAX #:030328), Ai9 (JAX #:007909), floxed-hM4Di (JAX #:026219), and Phox2b-Cre (JAX #:016223) mice were obtained from the Jackson Laboratory as congenic strains on the C57BL/6 J background. KRT14-CreER (JAX #:005107), Ai166 (JAX #:035404), and Ai195 (JAX #:034112) were obtained from the Jackson Laboratory on a mixed background. Hoxb8-FLPo mice (31) were generously provided by Victoria Abraira and Mahon Bohic (Rutgers University). Genotypes were confirmed by PCR using the protocol and primers listed on the JAX website. Both male and female mice were studied. Animals were separated by sex at weaning and group housed at 3-5 animals per cage. Only virgin animals were used for experiments. All mice were fed a standard diet unless otherwise noted (to receive doxycycline) and housed in standard cages, and were maintained on a 12-hour light/dark cycle.

Nail Trimming. To eliminate scratching-induced skin damage in the experiment shown in Fig. 1*D*, nail trimming was performed. To trim the nails, we restrained the mice in a 50 ml conical tube, which we modified to allow access to the hindlimbs during restraint. All nails were clipped on each hindlimb weekly for 7 wk with Spencer scissors (FST14076-09). Scratching analysis was performed as described below.

Doxycycline Administration. Doxycycline chow 200 mg/kg was purchased from Bio-Serv (S3888) and stored at 4 °C. Dox chow was offered to mice *ad libitum,* and the chow was refreshed every 2 wk with Dox chow from storage. To breeding females, the doxycycline chow began before mating and continued through to weaning. For postphenotypic Dox, mice that never received Dox and displayed lesions >20 mm^2 were administered Dox ad libitum for 2 mo.

Measurement of Mouse Behavior. The experimenter was blinded to the extent possible for all mouse behavior experiments. Mice were acclimatized to the behavior room and habituated to the experimental apparatus for 30 min for 3 straight days. Chemical injections were performed with a 30G hypodermic needle. The data presented in Fig. 1*E* display measurements collected from probing the shoulder skin. Fig. 1*J* and *SI Appendix*, Fig. S1*D* show behavioral assessments conducted after injections administered to the cheek. *SI Appendix*, Figs. S1 *E–G* and S6 *F* and *G* are from tests performed on the hind paws.

Documenting scratching. Mice were acclimatized as above, placed in opaque white cylinders over a platform, and recorded via an ImagingSource camera (DMK 37BUX252, lens TCSL0418 5MP) for 15 or 30 min in the dark. In some settings, mice were recorded with a handheld Sony video camera on a mirrored platform for a similar duration. Scratching bouts were scored on video playback and were defined as a single hindpaw motion that contacts either the cheek or the shoulder/back. The end of a bout was defined when the hindpaw was lowered.

Chloroquine-induced scratching. Mice were acclimatized for 30 min, and then 200 μg of chloroquine (Sigma 1650000) was injected intradermally into the cheek or intralesional area of the shoulder or in a comparable area in a Cre negative mouse without lesions. Scratching was measured for 30 min, as described above.

Von Frey measurement of mechanical sensitivity. For all groups, we recorded 3 d of baseline mechanical sensitivity. Animals were habituated on a wire mesh for 2 h, after which we used von Frey filaments (sizes 1.65, 2.44, 2.84, 3.22, 3.61, 3.84, 4.08, and 4.31) to measure mechanical withdrawal thresholds, using the up–down method. These filaments correspond to the following weights: 0.008, 0.004, 0.07, 0.16, 0.4, 0.6, 1, and 2 g, respectively.

Capsaicin-induced nocifensive behaviors. Mice were acclimatized for 30 min, and then 20 μg of capsaicin (Sigma M2028) in 20 μL of 7% Tween-80, 10% ethanol in PBS was injected intradermally into the cheek. Wiping was measured for 30 min in a setting comparable to that used to analyze scratching (48).

Hargreaves measurement of heat sensitivity. We acclimatized the mice for 30 min in Plexiglass cylinders. The mice were then placed on the glass of a Hargreaves apparatus, and the latency to withdraw the hind paw from the heat source was recorded. Each paw was tested five times, and we averaged latencies over the five trials. Hargreaves tests were done 1 h after the von Frey measurement.

Acetone-induced measurement of cold sensitivity. Mice were habituated for 30 min on a mesh in plexiglass cylinders. Next, we used a syringe to squirt 50 μl of acetone onto the plantar surface of the hind paw. The responses of the mice directly after the application of acetone were recorded on video for 30 s. Each paw was tested five times, and we measured events spent lifting, licking, or flinching the paw. Results are displayed as the total events across the five trials.

Assessment of skin lesion size. Skin lesions were defined as erosive (loss of epidermis) regions of unshaved mice. The maximum width and length of the lesions were measured with a digital caliper (Rexbeti).

Chemical Agents and Delivery. For acute drug experiments, a baseline measure of scratching was initially recorded over 30 min. 24 h later, scratching over 30 min was recorded with the drug on board, generating paired data points for each individual.

Gabapentin (*Sigma G154*) was injected intraperitoneally at 30 mg/kg after 30 min of acclimatization in the test chamber. Mouse behavior was measured 30 min after injection for another 30 min.

Nalfurafine was injected intraperitoneally at 20 μg/kg after 30 min of acclimatization. Mouse behavior was measured 30 min after injection for another 30 min.

Morphine (Sigma M8777) was injected intraperitoneally at 10 mg/kg after 30 min of acclimatization. Mouse behavior was measured 30 min after injection for another 30 min.

Cetirizine (Sigma BP837) was injected intraperitoneally at 30 mg/kg after 30 min of acclimatization. Mouse behavior was measured 30 min after injection for another 30 min.

Resiniferatoxin (Adipogen AG-CN2-0534-MC01) was diluted at 1.0 mg/ml in 100% ethanol and then subcutaneously injected with 3 escalating consecutive daily doses of 30, 60, and 100 mg/kg in 300 μL of normal saline. The efficacy of RTX-mediated TRPV1+ sensory nerve ablation was assessed by monitoring tail-flick latency, which increased to a 15-s cut-off.

Clozapine-N-oxide (Cayman Chemical) was added to a solution of 5.0 mg CNO in 40 mL of PBS. This solution was topically painted on the skin every day for 10 d, unilaterally over the skin lesion; the contralateral skin lesion received a similar volume of PBS.

Tamoxifen Administration in KRT14-CreER Mice. *For topical application: 4-hydroxy-Tamoxifen* (Sigma-Aldrich) was dissolved in ethanol (1.0 mg/50 ml) at 55 degrees for 15 min with vortexing, and aliquots were stored at −20 degrees. First, the mouse was anesthetized using ketamine (80 mg/kg ketamine + 5.0 mg/kg xylazine). Next, both sides of the mouse, spanning from the ear to the lower abdomen, were depilated with Nair, creating two lateral stripes down the back, preserving fur at the dorsal midline. A total of 100 μL of the 4-OHT solution was applied on the right side of the depilated skin using a micropipette. Small droplets of the solution were dispensed and rubbed equally across the depilated area. On the left side, 100 μL of ethanol (vehicle) was similarly applied. Mice were monitored in a holding cage until they were ambulatory and then returned to their home cage; their general health was monitored daily. The liquid application, but not the Nair, was repeated for three days.

For *systemic administration:* Tamoxifen (Sigma Cat #5648) 100 mg/kg in corn oil (Sigma Cat #8267) was injected intraperitoneally. This dose was repeated every other day for a total of three injections. Mice were returned to their home cage after injection, and their general health was monitored daily.

6-OHDA Induced Sympathectomy. Mice were intraperitoneally injected with 100 mg/kg 6-OHDA in 0.01% ascorbic acid in PBS once (vehicle is 0.01% ascorbic acid in PBS). Mice were returned to their home cage after injection, and their general health was monitored daily. A measurement of scratching frequency was taken at 1 mo postinjection.

Cutaneous Surgical Denervation. 6 wk Phox2a-Cre; Ai162 mice (N = 4, 3 female) with established scratching and skin lesions were anesthetized with ketamine/xylazine, before receiving a dorsal midline skin incision at the upper back. Following a previous protocol (49), the skin on the right side was reflected to expose the cutaneous nerves. Unilateral surgical denervation was performed by carefully isolating and transecting the upper thoracic-level cutaneous nerves at their skin entry points, while avoiding blood vessels. On the contralateral side, a sham operation was performed where the skin was similarly reflected, but the cutaneous nerves were left intact. The incision was closed with 5-0 monocryl sutures, and mice were allowed to recover on a heating pad. Animals were measured for scratching 4 d after this procedure.

qPCR. In tamoxifen-injected KRT14-CreER; Ai162 mice and littermate Cre negative controls, a ventral 2x2 cm patch of skin was harvested. The epidermis was separated from the whole skin by incubating in Trypsin-EDTA 0.15% for 45 min. Isolated cells from the epidermis and whole mRNA was extracted using an RNeasy Mini kit from Qiagen after which was reverse transcribed into cDNA using Superscript IV (ThermoFisher Cat # 18091200). qPCR analyses were carried out with gene specific primers and fluorescently labeled Taqman probes (ThermoFisher Scientific) for Tslp (Mm01157588_m1), Il33 (Mm00505403_m1), Edn1 (Mm00438659_m1), and Postn (Mm01284919_m1). Relative expression level was calculated using the $2 - \Delta\Delta CT$ method. β-actin (Mm02619580_g1) was used as the internal control for each sample.

Histology. For histology of whole mount samples (DRGs, spinal cord, and skin), mice were transcardially perfused with phosphate-buffered 4% formalin. Then the spinal column and a section of the skin of the upper back were dissected and stored in 4% formalin overnight. After washing with PBS, DRGs and the spinal cord were manually extracted from the spinal column. In a few cases, a pregnant dam was perfused with 4% formalin near term to obtain embryos for whole-body tissue analysis. The embryos were extracted after perfusion and then postfixed in 4% formalin for 24 h and stored in PBS.

For histology of samples, the spinal cord was sectioned using a cryostat or freezing microtome at 50-micron or 100-micron thickness. Sections were stored in PBS after sectioning. Generally, the fluorescence of GCaMP6 or tdTomato was detected without antibody labeling. However, some DRG and spinal cord sections were counterstained with Neurotrace (N21479, ThermoFisher) or DAPI (D1306, ThermoFisher) to label cell bodies. For phospho-ERK1/2 and GFP immunolabeling, sections were first blocked with 10% Normal Goat Serum (NGS) in 0.08% Triton-X in Phosphate Buffered Saline (PBT) overnight, and then incubated in a primary antibody solution of 1:1000 pERK antibody (#4370, Cell Signaling Technology) and 1:2,000 GFP antibody (#ab13970, Abcam) in 5% NGS PBT overnight, then washed three times with PBT, and then incubated in a secondary antibody solution of 1:1,000 anti-Rabbit Alexa-647 (#A-21246, ThermoFisher Scientific) and 1:1000 anti-Chicken Alexa-488 (#A-11039, ThermoFisher Scientific) in PBT overnight, then washed three times with PBT before mounting. Sections were mounted onto glass slides using Fluoromount mounting media (00-4958-02, ThermoFisher) and a no.1.5 glass coverslip. Imaging of the expression of tdTomato or GCaMP6 in spinal cord or brain sections was acquired using confocal microscopy. Specifically, an FV3000 system with LED laser illumination, Standard Detectors, and a 4X (NA 0.16) and 10X (NA 0.4) lens was used to acquire z-stacks (1AU slices) or single planes (wide pinhole, 8X AU). Whole mount skin and embryos were imaged using an Axio Zoom V16 outfitted with a 1X objective (NA 0.25), which provided a large FOV, and an AxioCam 712 and Excelitas Xylis light source. In the sample from a doxycycline-rescued Phox2a; Ai166 mouse, the intact brain and spinal cord were cleared using Life Canvas technologies SHIELD clearing reagents and imaged on a smartSPIM (LifeCanvas) light-sheet microscope following established protocols (50).

Histological Counts of Cervical Spinal Neurons. 50-micron transverse cryostat sections of the entire cervical enlargement were collected. A regularly spaced subset of sections (one every 150 microns) was selected for DAPI staining and mounted. All selected sections were imaged for endogenous tdTomato and DAPI at 1.6 × 1.6 × 8-micron resolution with eight z-slices using a 10X objective on an FV3000 confocal. Cell counting was performed on at least 3 sections per mouse and averaged. An unpaired *t* test between groups was performed in Prism. For a cell to be counted, it had to meet the criteria of having a rounded cell body represented in the z-stack and a DAPI-labeled nucleus. Cell counting was performed blind to the independent variable (tTA genotype) using the Cell Counter plugin in ImageJ (FIJI).

Whole Mount Skin Collection. After intracardiac perfusion with 4% PFA fixative, the skin around the shoulder, including the ear, was dissected and kept for 24 h in fixative. After 24 h, the skin tissue was washed in PBS twice and stored in PBS until imaging. Usually, the fur was shaved before perfusion using an electric clipper.

Fate Mapping. In Ai9 mice, cellular tdTomato reporter expression is evidence of a Cre recombination event in that cell or in any of its ancestors. We examined the brain, spinal cord, skin, whole body, and embryonic expression of tdTomato in Phox2a-Cre mice or Phox2b-Cre mice to generate a fate map. For this report, we focused on the nervous system and skin.

Data Presentation. Various schematics describing experiments or fate mapping results were created with BioRender.com. Data were compiled and graphed in GraphPad Prism9. Figures were generated in Adobe Photoshop 2024. Statistical tests were performed in Prism9. Statistical analysis of differences between groups was performed using Student's *t* test (unpaired for comparison between two groups or paired for treatments performed in the same mouse). qPCR data were analyzed using a Mann–Whitney test. Data were considered significantly different at $P \leq 0.05$. Group data in bar graphs, scatter, or line plots are expressed as means, with error bars representing the 95% CI.

Data, Materials, and Software Availability. Primary imaging data are available via Dryad Data Repository (51). Primary numerical data for all graphs and statistics in the main text and *SI Appendix* have been deposited in the Dryad Data Repository (Dataset DOI: 10.5061/dryad.tdz08kq9s) (51). All other data are included in the article and/or supporting information.

ACKNOWLEDGMENTS. This work was supported by NIH NSR35097306 (A.I.B.), Open Philanthropy (A.I.B.), NIH F32 5F32DE029384 (A.J.C.), Canadian Institutes of Health Research (PJT-162225, MOP-77556, PJT-153053, and PJT-159839) (A.K.), NSF Graduate Research Fellowship 2034836 (M.R.C.), and a Dermatology Foundation Career Development Award, Investigator Research Fellowship, Sandler Foundation Program in Breakthrough Biomedical Research and NIH-5T32AR007175 (S.W.K.). Special thank you to the UCSF Laboratory Animal Resource Center veterinarians, rodent vet nurses, and the entire rodent health team for supervising the health of the animals used in this study.

1. K. E. Sadler, F. Moehring, C. L. Stucky, Keratinocytes contribute to normal cold and heat sensation. *eLife* **9**, e58625 (2020).
2. K. M. Baumbauer *et al.*, Keratinocytes can modulate and directly initiate nociceptive responses. *eLife* **4**, e09674 (2015).
3. J. Schwendinger-Schreck, S. R. Wilson, D. M. Bautista, Interactions between keratinocytes and somatosensory neurons in itch. *Handb. Exp. Pharmacol.* **226**, 177–190 (2015).
4. J. J. Emrick *et al.*, Tissue-specific contributions of Tmem79 to atopic dermatitis and mast cell-mediated histaminergic itch. *Proc. Natl. Acad. Sci. U. S. A.* **115**, E12091–E12100 (2018).
5. D. M. Bautista, S. R. Wilson, M. A. Hoon, Why we scratch an itch: The molecules, cells and circuits of itch. *Nat. Neurosci.* **17**, 175–182 (2014).
6. P.-Y. Tseng, M. A. Hoon, GPR15L is an epithelial inflammation-derived pruritogen. *Sci. Adv.* **8**, eabm7342 (2022).
7. S. K. Mishra *et al.*, Periostin activation of integrin receptors on sensory neurons induces allergic itch. *Cell Rep.* **31**, 107472 (2020).
8. S. R. Wilson *et al.*, The epithelial cell-derived atopic dermatitis cytokine TSLP activates neurons to induce itch. *Cell* **155**, 285–295 (2013).
9. X. Dong, X. Dong, Peripheral and central mechanisms of itch. *Neuron* **98**, 482–494 (2018).
10. A. Ikoma, M. Steinhoff, S. Ständer, G. Yosipovitch, M. Schmelz, The neurobiology of itch. *Nat. Rev. Neurosci.* **7**, 535–547 (2006).
11. S. K. Mishra, S. M. Tisel, P. Orestes, S. K. Bhangoo, M. A. Hoon, TRPV1-lineage neurons are required for thermal sensation: TRPV1-lineage neurons. *EMBO J.* **30**, 582–593 (2011).
12. O. Mahmoud, G. B. Soares, G. Yosipovitch, Transient Receptor Potential channels and itch. *Int. J. Mol. Sci.* **24**, 420 (2022).
13. A. I. M. van Laarhoven *et al.*, Itch sensitization? A systematic review of studies using quantitative sensory testing in patients with chronic itch. *Pain* **160**, 2661–2678 (2019).
14. O. Mahmoud, O. Oladipo, R. H. Mahmoud, G. Yosipovitch, Itch: From the skin to the brain - peripheral and central neural sensitization in chronic itch. *Front. Mol. Neurosci.* **16**, 1272230 (2023).
15. B. Ahanonu, A. Crowther, A. Kania, M. Rosa-Casillas, A. I. Basbaum, Long-term optical imaging of the spinal cord in awake behaving mice. *Nat. Methods* **21**, 2363-2375 (2024).
16. A. Cowan, G. B. Kehner, S. Inan, Targeting itch with ligands selective for κ opioid receptors. *Handb. Exp. Pharmacol.* **226**, 291–314 (2015).
17. T. A. Leslie, M. W. Greaves, G. Yosipovitch, Current topical and systemic therapies for itch. *Handb. Exp. Pharmacol.* **226**, 337–356 (2015).
18. J. C. Ballantyne, A. B. Loach, D. B. Carr, Itching after epidural and spinal opiates. *Pain* **33**, 149–160 (1988).
19. S. Inan, A. Cowan, Antipruritic effects of kappa opioid receptor agonists: evidence from rodents to humans. *Handb. Exp. Pharmacol.* **271**, 275–292 (2022).
20. T. Akiyama, M. I. Carstens, D. Piecha, S. Steppan, E. Carstens, Nalfurafine suppresses pruritogen- and touch-evoked scratching behavior in models of acute and chronic itch in mice. *Acta Derm. Venereol.* **95**, 147–150 (2015).
21. S. E. Ross *et al.*, Loss of inhibitory interneurons in the dorsal spinal cord and elevated itch in Bhlhb5 mutant mice. *Neuron* **65**, 886–898 (2010).
22. M. B. Veldman *et al.*, Brainwide genetic sparse cell labeling to illuminate the morphology of neurons and glia with Cre-dependent MORF mice. *Neuron* **108**, 111–127.e6 (2020).
23. E. Coppola, F. d'Autréaux, F. M. Rijli, J.-F. Brunet, Ongoing roles of Phox2 homeodomain transcription factors during neuronal differentiation. *Development* **137**, 4211–4220 (2010).
24. R. B. Roome *et al.*, Phox2a defines a developmental origin of the anterolateral system in mice and humans. *Cell Rep.* **33**, 108425 (2020).
25. W. A. A. Alsulaiman *et al.*, Characterisation of lamina I anterolateral system neurons that express Cre in a Phox2a-Cre mouse line. *Sci. Rep.* **11**, 17912 (2021).
26. D. Piyush Shah, A. Barik, The spino-parabrachial pathway for itch. *Front. Neural Circuits* **16**, 805831 (2022).
27. X. Ren *et al.*, Identification of an essential spinoparabrachial pathway for mechanical itch. *Neuron* **111**, 1812–1829.e6 (2023).
28. V. Vasioukhin, L. Degenstein, B. Wise, E. Fuchs, The magical touch: Genome targeting in epidermal stem cells induced by tamoxifen application to mouse skin. *Proc. Natl. Acad. Sci. U. S. A.* **96**, 8551–8556 (1999).
29. A. M. Trier *et al.*, IL-33 signaling in sensory neurons promotes dry skin itch. *J. Allergy Clin. Immunol.* **149**, 1473–1480.e6 (2022).
30. M. Kido-Nakahara *et al.*, Neural peptidase endothelin-converting enzyme 1 regulates endothelin 1-induced pruritus. *J. Clin. Invest.* **124**, 2683–2695 (2014).
31. M. Bohic *et al.*, A new Hoxb8FlpO mouse line for intersectional approaches to dissect developmentally defined adult sensorimotor circuits. *Front. Mol. Neurosci.* **16**, 1176823 (2023).
32. A. Fernández-Carvajal, G. Fernández-Ballester, A. Ferrer-Montiel, TRPV1 in chronic pruritus and pain: Soft modulation as a therapeutic strategy. *Front. Mol. Neurosci.* **15**, 930964 (2022).
33. N. Imamachi *et al.*, TRPV1-expressing primary afferents generate behavioral responses to pruritogens via multiple mechanisms. *Proc. Natl. Acad. Sci. U.S.A.* **106**, 11330–11335 (2009).
34. A. W. Liu *et al.*, Scratching promotes allergic inflammation and host defense via neurogenic mast cell activation. *Science* **387**, eadn9390 (2025).
35. F. Moehring *et al.*, Keratinocytes mediate innocuous and noxious touch via ATP-P2X4 signaling. *eLife* **7**, e316684 (2018).
36. A. R. Mikesell *et al.*, Keratinocyte PIEZO1 modulates cutaneous mechanosensation. *eLife* **11**, e65987 (2022).
37. A. Latremoliere, C. J. Woolf, Central sensitization: A generator of pain hypersensitivity by central neural plasticity. *J. Pain* **10**, 895–926 (2009).
38. G. Yosipovitch, E. Carstens, F. McGlone, Chronic itch and chronic pain: Analogous mechanisms. *Pain* **131**, 4–7 (2007).
39. K. Bannister *et al.*, Multiple sites and actions of gabapentin–induced relief of ongoing experimental neuropathic pain. *Pain* **158**, 2386–2395 (2017).
40. R. Baron, G. Hans, A. H. Dickenson, Peripheral input and its importance for central sensitization. *Ann. Neurol.* **74**, 630–636 (2013).
41. N. A. Steinmetz *et al.*, Aberrant cortical activity in multiple GCaMP6-expressing transgenic mouse lines. *eNeuro* **4**, ENEURO.0207-17.2017 (2017).
42. S. Papaioannou, P. Medini, Advantages, pitfalls, and developments of all optical interrogation strategies of microcircuits in vivo. *Front. Neurosci.* **16**, 859803 (2022).
43. S. Teng *et al.*, Expression of GCaMP6s in the dentate gyrus induces tonic–clonic seizures. *Sci. Rep.* **14**, 1–12 (2024).
44. Y. Yang *et al.*, Improved calcium sensor GCaMP-X overcomes the calcium channel perturbations induced by the calmodulin in GCaMP. *Nat. Commun.* **9**, 1504 (2018).
45. M. P. Pedro, K. Lund, R. Iglesias-Bartolome, The landscape of GPCR signaling in the regulation of epidermal stem cell fate and skin homeostasis: Regulation of epidermal stem cell fate by GPCRs. *Stem. Cells* **38**, 1520–1531 (2020).
46. M. P. Pedro, N. Salinas Parra, J. S. Gutkind, R. Iglesias-Bartolome, Activation of G-protein coupled receptor-Gαi signaling increases keratinocyte proliferation and reduces differentiation, leading to epidermal hyperplasia. *J. Invest. Dermatol.* **140**, 1195–1203.e3 (2020).
47. M. P. Pedro *et al.*, GPCR screening reveals that the metabolite receptor HCAR3 regulates epithelial proliferation, migration, and cellular respiration. *J. Invest. Dermatol.* **144**, 1311–1321.e7 (2024).
48. S. G. Shimada, R. H. LaMotte, Behavioral differentiation between itch and pain in mice. *Pain* **139**, 681–687 (2008).
49. S. C. Peterson, I. Brownell, S. Y. Wong, Cutaneous surgical denervation: A method for testing the requirement for nerves in mouse models of skin disease. *J. Vis. Exp.* **112**, 54050 (2016), 10.3791/54050.
50. Y.-G. Park *et al.*, Protection of tissue physicochemical properties using polyfunctional crosslinkers. *Nat. Biotechnol.* **37**, 4281 (2018), 10.1038/nbt.4281.
51. A. J. Crowther, Data for: Keratinocyte-TRPV1 sensory neuron interactions in a genetically controllable mouse model of chronic neuropathic itch. Dryad Data Repository. https://doi.org/10.5061/dryad.tdz08kq9s. Deposited 27 May 2025.